



Impact of 1, 2 and 4 °C of global warming on ship navigation in the Canadian Arctic

Lawrence R. Mudryk¹✉, Jackie Dawson², Stephen E. L. Howell¹, Chris Derksen¹, Thomas A. Zagon³ and Mike Brady¹

Climate change-driven reductions in sea ice have facilitated increased shipping traffic volumes across the Arctic. Here, we use climate model simulations to investigate changing navigability in the Canadian Arctic for major trade routes and coastal community resupply under 1, 2 and 4 °C of global warming above pre-industrial levels, on the basis of operational Polar Code regulations. Profound shifts in ship-accessible season length are projected across the Canadian Arctic, with the largest increases in the Beaufort region (100–200 d at 2 °C to 200–300 d at 4 °C). Projections along the Northwest Passage and Arctic Bridge trade routes indicate 100% navigation probability for part of the year, regardless of vessel type, above 2 °C of global warming. Along some major trade routes, substantial increases to season length are possible if operators assume additional risk and operate under marginally unsafe conditions. Local changes in accessibility for maritime resupply depend strongly on community location.

Over 90% of goods traded internationally are shipped by sea¹, which accounts for ~40% of the entire global economy². Maritime trade (the movement of goods) and transportation (the movement of people) support every economic sector worldwide and play a substantial role in underpinning economic growth, improving social conditions, reducing risks to human health and contributing to poverty alleviation^{3–5}. Global ship traffic flows predominantly via the Panama and Suez Canals but climate change reductions in sea ice are projected to increase the navigability across the Arctic through the Northwest Passage, Northern Sea Route and Transpolar Sea Route^{6–8} (Fig. 1a). A more accessible Arctic will create new opportunities for shorter, potentially more economical, northern maritime trade routes imagined by global leaders for centuries.

The Canadian Arctic represents a key region for trans-Arctic shipping because of the presence of the Northwest Passage and Arctic Bridge trade routes (Fig. 1b). There are also many northern communities culturally and economically connected to these routes, which rely on maritime traffic for resupply^{9,10}. Over the past five decades, sea ice extent in the Canadian Arctic has decreased by 5–20% per decade (depending on region) during the summer months with notable reductions in the proportion of multi-year ice^{11,12}. Concurrently, the distance travelled by ships through the region has increased threefold¹³. Changes in ship traffic are primarily driven by increased access to natural resources including mines and fisheries^{14,15}, as well as tourism opportunities^{16–18} and burgeoning desires for trans-Arctic trade^{19,20}.

Several studies have investigated the probability of a sea ice-free Arctic in the summer under different global warming thresholds^{21–24} but important gaps still exist with respect to understanding how ship navigability may change as a consequence of sea ice reductions. Sea ice ‘free’ by definition refers to total Arctic sea ice extent that is <1 million km², which is not directly relevant at the ship scale nor at the community level where the impacts of both changing ice conditions and increased shipping traffic will be felt. Furthermore,

since 2015 and the adoption of the United Nations Framework Convention on Climate Change (UNFCCC) Paris Agreement, which binds signatory nations to a collective goal of keeping global temperature increase to below 2 °C above pre-industrial levels, it has become increasingly important for studies to evaluate projections on the basis of degrees warming instead of difficult-to-compare Representative Concentration Pathways. Existing studies projecting shipping navigability changes in the Arctic^{7,8} have not considered globally relevant temperature targets. This is an important omission in the literature since an understanding of how Arctic accessibility changes as a function of real-world policy thresholds is needed to support coordinated international decision-making. In response to these needs, we project changes in Arctic navigability across a range of projected warming spanning 1, 2 and 4 °C above pre-industrial levels while also providing information at progressive levels of spatial granularity: (1) across Arctic Canada, (2) in regions relevant to specific shipping routes and (3) at the scales relevant to specific Arctic communities. We intend the results to support a broad range of policy decisions (for example, future trade route development and community resupply). While our focus here is on sea ice as a physical barrier to navigation that sets the broadest-scale constraints on shipping, the future of Arctic shipping will also depend on a wide array of social, economic and political factors, as we highlight and connect to our results in the Discussion.

We use a single model initial condition large ensemble of climate simulations (Methods) to project changes in sea ice at various thresholds of warming (1, 2 and 4 °C) above the global mean pre-industrial value. We present results in terms of warming thresholds since the mean Arctic sea ice response is directly related to the global mean surface temperature and thereby to global cumulative carbon emissions^{25–28}. A particular warming threshold therefore provides a way to index change in climate conditions roughly independently of the particular emissions scenario used in the simulations^{25,26,29–31}. This change in framework from examining a particular pathway of future emissions to indexing global

¹Climate Research Division, Environment and Climate Change Canada, Toronto, Ontario, Canada. ²Department of Geography, Environment, and Geomatics, University of Ottawa, Ottawa, Ontario, Canada. ³Canadian Ice Service, Environment and Climate Change Canada, Ottawa, Ontario, Canada. ✉e-mail: lawrence.mudryk@canada.ca

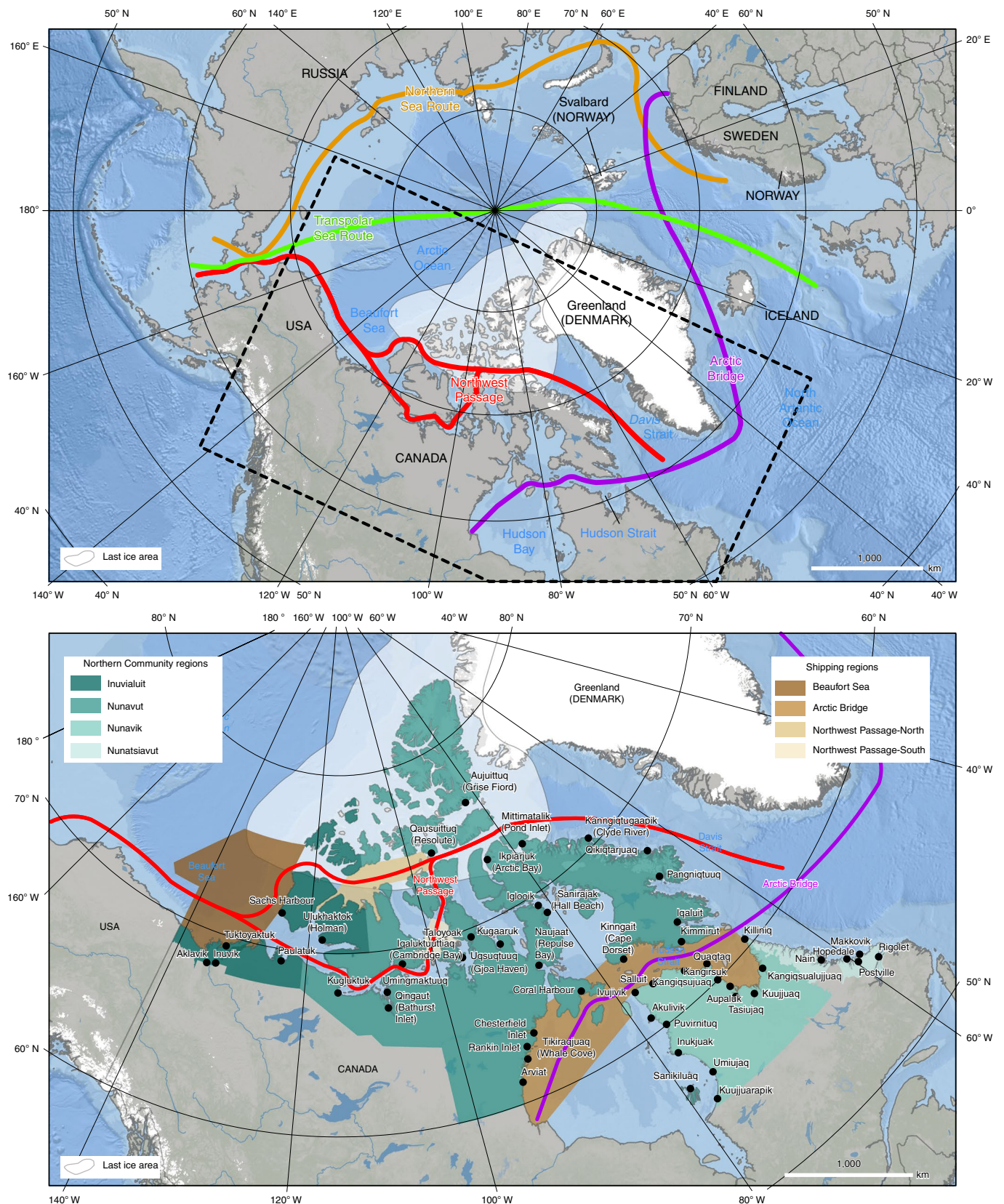


Fig. 1 | Trans-Arctic and Canadian shipping routes. a, Trans-Arctic routes and location of the LIA. **b,** Canadian Arctic shipping regions of interest (brown shading), Northern Community regions (green shading) and population centres (labelled). Basemap credit: Esri, GEBCO, DeLorme, NaturalVue, Garmin, NOAA NGDC and others.

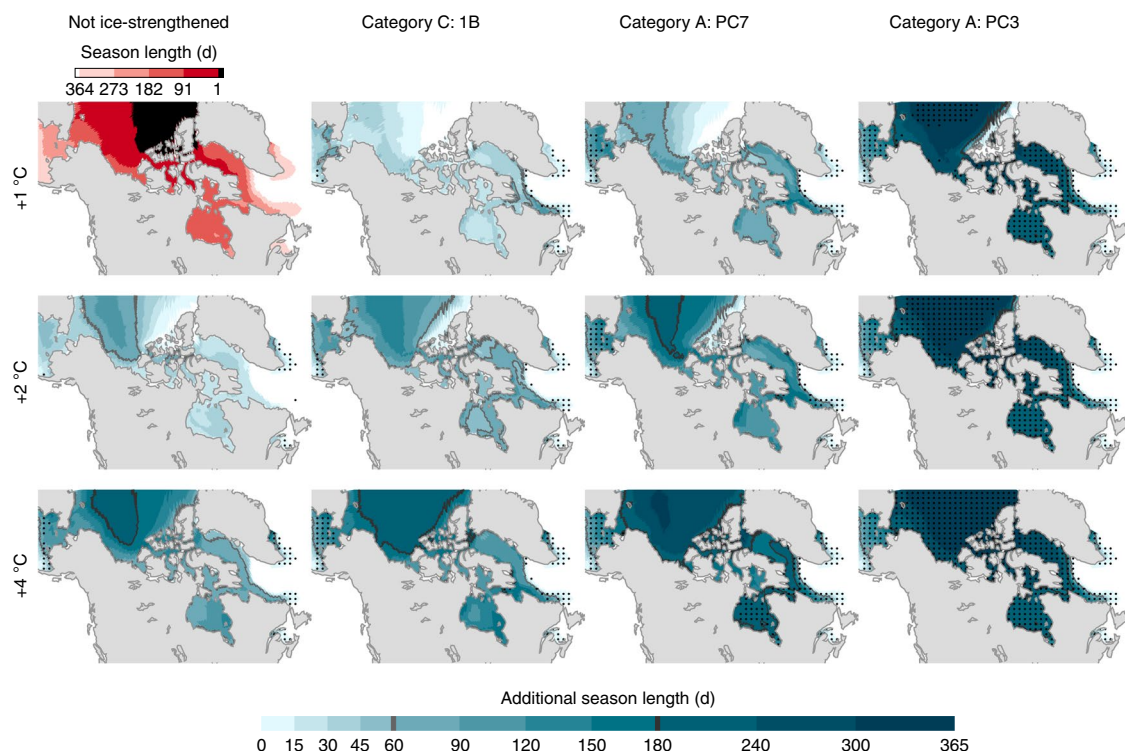


Fig. 2 | Present-day and projected changes in shipping season length for various vessel classes. Present-day climatological season length (simulated) for non-ice-strengthened vessels (pleasure craft) shown at upper left (approximately +1 °C above pre-industrial level). Relative differences for ice-strengthened classes (columns) and additional warming relative to pre-industrial level (rows) shown using scale at bottom. Differences of 60 and 180 d are highlighted. Stippling marks regions where the season length is >360 d per year. Season length uses RIO ≥ 0 as the threshold for safe navigation, as described in Methods.

temperature rise is also directly in line with policy-focused thresholds determined by the UNFCCC Paris Agreement³². From the projected sea ice conditions at various warming thresholds, we calculate the resulting impact on shipping by converting sea ice thickness into Risk Index Outcome (RIO) values (Methods). This conversion allows the model output to be directly interpretable within the Polar Operational Limit Assessment Risk Index System (POLARIS)³³ under the International Maritime Organization's Polar Code³⁴ used by ship operators to determine go/no-go areas on the basis of ice risk. The Polar Code entered into force on 1 January 2017, extending the requirements of the SOLAS and MARPOL Conventions to account for the unique climatic conditions of polar waters^{34–36}. We compare the impact of sea ice change on navigational limits by examining changes in season length and timing for the general Canadian Arctic region, for its major maritime trade routes (Northwest Passage and Arctic Bridge) and along resupply routes to coastal communities. Our analysis considers season length changes among four different vessel classes: Category A Polar Class 3 vessels (PC3; year-round operation in first- and second-year ice with some multi-year ice present) typically used for ice breaking; Category A Polar Class 7 vessels (PC7; summer/autumn operation in first-year ice with some second-year ice present), typically used for community resupply operations; Category C 1B vessels (1B; thin and new ice only), typical of expedition-style passenger vessels and some resupply operations; and non-ice-strengthened vessels (NIS) typical of private yachts or pleasure craft.

Navigability changes across the Canadian Arctic

The spatial distribution of projected changes to operational shipping season length in the Canadian Arctic for ship classes NIS (for example, pleasure craft), 1B (for example, cruise ship), PC7

(for example, resupply ships) and PC3 (for example, ice breakers) under 1, 2 and 4 °C of global warming are shown in Fig. 2. While there is strong dependence between the magnitude of warming and projected changes in shipping season length, there are important regional differences and large differences between vessel classes.

The Beaufort Sea region experiences the most dramatic lengthening of the shipping season for all vessel types, increasing from 100–200 d at 2 °C to 200–300 d at 4 °C. This large increase is primarily the result of the projected transition from a perennial multi-year ice regime to a seasonal first-year ice regime under increased levels of global warming. Observations show that this change in predominant ice type is already well underway in the Beaufort Sea^{37,38}.

For ship classes 1B and higher, notable increases in the operational shipping season length occur in the Beaufort Sea and Arctic Ocean at 2 °C (60–150 d) and then increase dramatically at 4 °C warming (180–240 d). Increases for 1B vessels appear more modest within the Hudson Bay region under 2 and 4 °C of warming because the ice regime is already seasonal in this region (as it was under a pre-industrial climate) so there is a limit to the absolute increase in projected shipping season length.

At present levels of warming, PC3 and PC7 vessels are only restricted by the presence of the oldest and thickest sea ice in the world, which is located in the northern Canadian Arctic and to the north of Greenland. This region is referred to as the Last Ice Area (LIA) (Fig. 1) because sea ice is expected to persist here even when most Arctic Ocean is sea ice-free^{11,39}. Under 2 °C of warming for a PC3 vessel, year-round navigation is projected everywhere across the Canadian Arctic except the LIA. This is no longer the case at 4 °C of warming, by which point the entire Canadian Arctic is projected to be navigable for PC3 vessels. For PC7 vessels at 4 °C warming, projected ice conditions would allow travel through Hudson

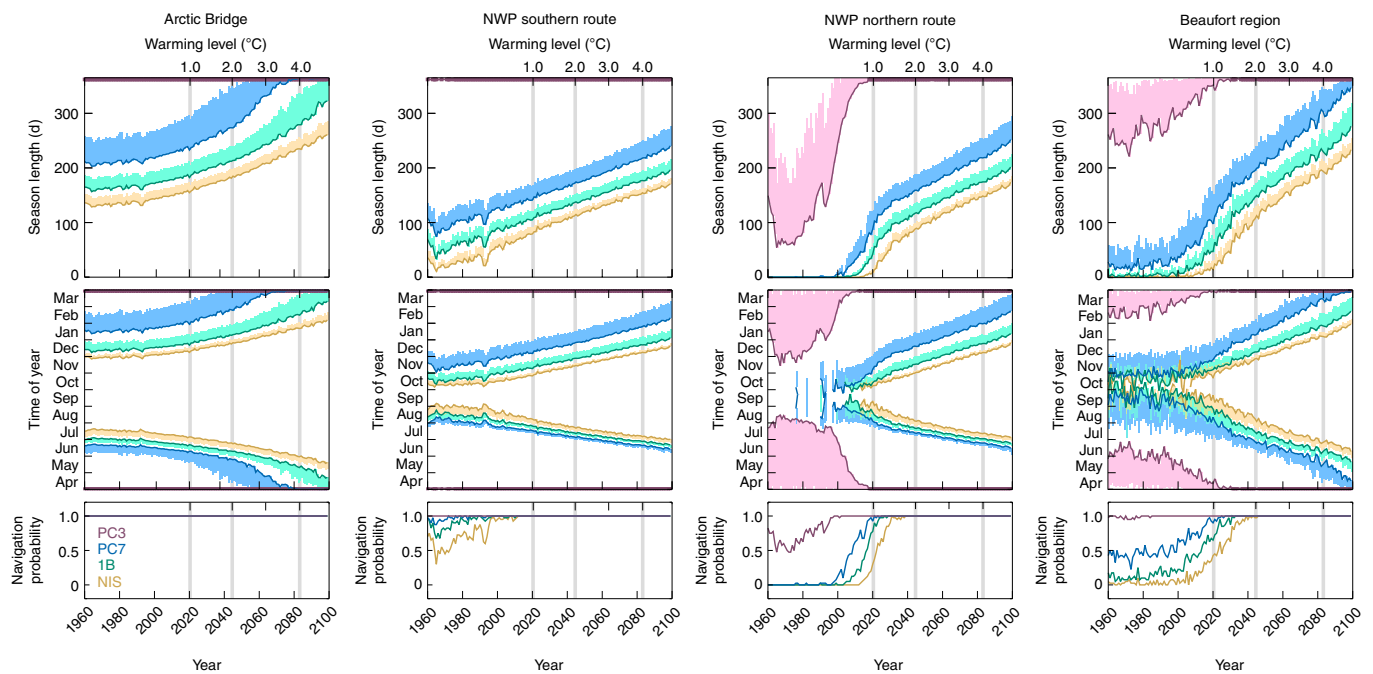


Fig. 3 | Evolution of navigability in four Canadian shipping regions. Season length (top row), first/last day of possible transit (middle row) and annual navigation probability (bottom row) shown across four selected Canadian shipping regions and for four ship classes: PC3 (magenta), PC7 (blue), 1B (green) and non-ice-strengthened (NIS; yellow). NWP, Northwest Passage. Solid lines show ensemble mean values for nominal risk (RIO = 0); shading shows increased season length and earlier opening/later closing of routes associated with enhanced risk ($-10 < \text{RIO} < 0$). Vertical grey lines indicate ensemble mean timing of 1, 2 and 4°C warming thresholds relative to pre-industrial values.

Bay and the Labrador Sea year-round. Year-round navigation will not be possible, however, for NIS or 1B class vessels even under 4°C warming because of the persistence of sea ice associated with the LIA.

Navigability changes for trade and transportation corridors

Evolution of projected shipping season length, timing of the season start and end and navigation probability for four trade and transportation corridors within Arctic Canada and for four ship classes are shown over 1960–2100 in Fig. 3. The trade corridors considered are the Beaufort Sea, the Northwest Passage (southern and northern routes) and the Arctic Bridge region as shown in Fig. 1. We consider the Beaufort Sea as it continues to be a focus region for resource extraction⁴⁰ and also represents the western entrance/exit of the Northwest Passage. With the construction of new interior roads to Tuktoyaktuk and increased ship navigability over its waters, this region has the potential to become a busier trade and transportation corridor in the future. By 2°C of warming (~2045), all major shipping routes indicate 100% navigation probability for part of the year regardless of vessel type. However, within the Beaufort and Northwest Passage regions of the Canadian Arctic Archipelago, a considerably shorter operational shipping season remains, even under 4°C of warming for all ship classes, with the exception of PC3 class ice-breaking vessels. Model uncertainty until mid-century is higher for the higher latitude regions of the Canadian Arctic Archipelago and the northern route of the Northwest Passage because of challenges in simulating multi-year ice in these transport corridors. Comprehensive comparisons with observed sea ice thicknesses^{41–43} indicate models tend to overestimate the historical thickness of multi-year ice. This bias implies that projected shipping impacts in these regions will be more uncertain at intermediate time scales (for example, 2°C of warming or ~2050). Over longer projection periods and greater warming, this uncertainty is reduced as the ice regime transitions to thinner, more seasonal ice cover.

Increased shipping season length in these regions is attributable to the gradual loss of multi-year ice, which is not projected to completely disappear even under 4°C warming. While current season lengths differ drastically among non-ice-breaking vessel types from a marginal 10 d for NIS vessels in the northern route to 150 d for PC7 vessels in the southern route, increases are projected to be approximately independent of vessel type. Compared to current season lengths, at 2°C global warming season length in the southern route is projected to increase by close to 30 d for PC7, 1B and NIS vessels, by about 75 d in the northern route and by 90–100 d in the Beaufort region. At 4°C global warming, season length increases are even greater: 70–80 d in the southern route and 130–140 d in the northern route. In the Beaufort region, increases of ~175 d are projected for 1B and NIS vessels and over 210 d for PC7 vessels. While season length increases during both shoulder seasons for all routes, the largest increases occur during the fall consistent with current observations⁴⁴. Differences in navigability among vessel type are also larger during the fall than the spring.

The Arctic Bridge is an important maritime route connecting Canada's only Arctic port to Europe and supporting grain exports from central Canada. The Port of Churchill, located at 58°N on the west coast of Hudson Bay is an international port with four loading berths and one tanker berth and is capable of handling large Panamax class vessels (60,000–80,000 t)⁴⁵. The Arctic Bridge is composed entirely of seasonal ice and thus the absolute shipping season increases are not as substantial as other corridors and regions. However, open water vessels making use of the Arctic Bridge are expected to have an ~250-d season length at 4°C warming and the route could facilitate year-round navigation for PC7 class vessels before 4°C warming.

Navigability changes for community resupply and tourism

Projected increases in navigability of PC7 (resupply) class ships servicing communities across the Canadian Arctic under 2 and 4°C of

Northern Community increases in supply ship navigability

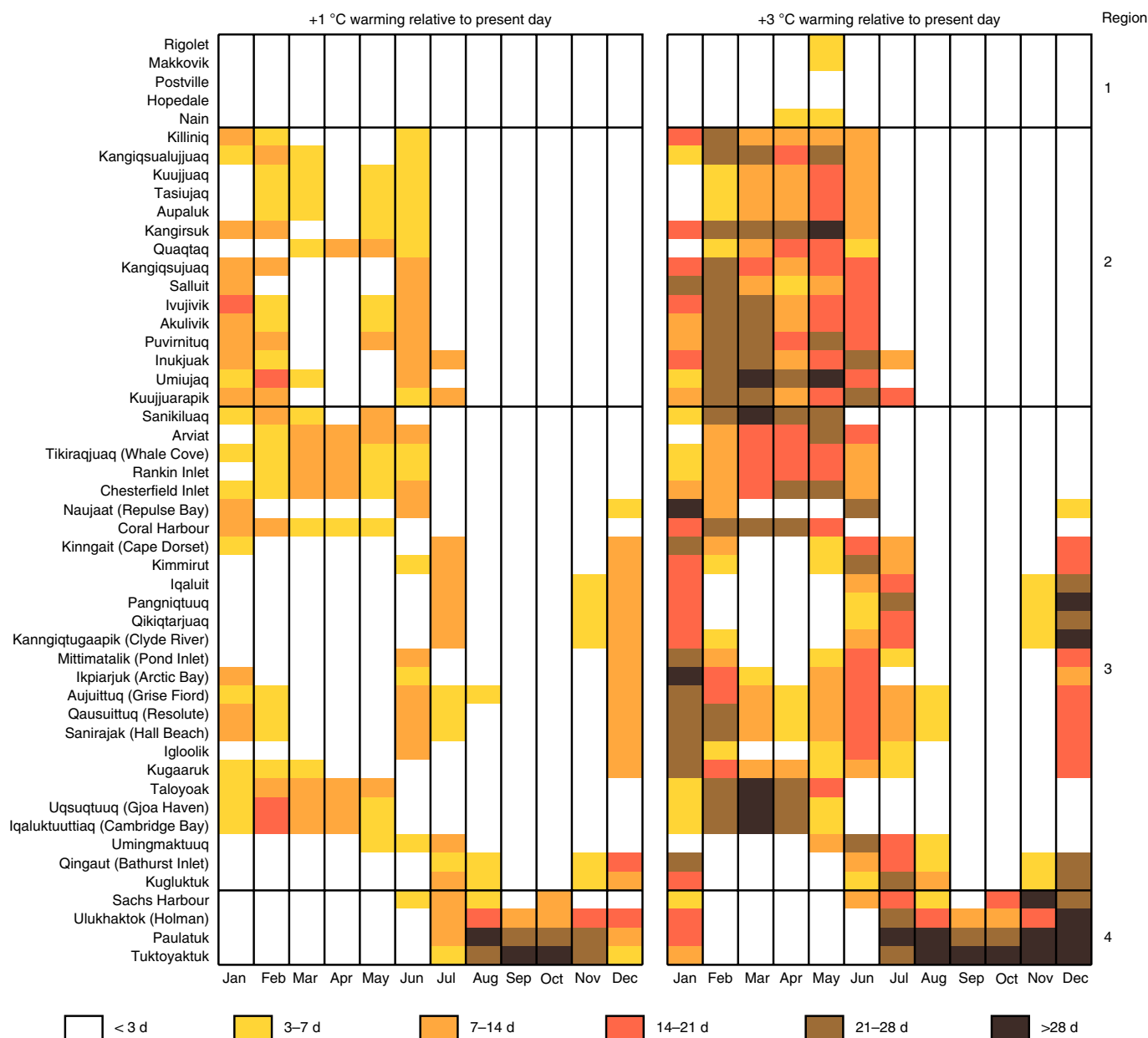


Fig. 4 | Changes in timing of supply ship navigability for localized regions of Northern Communities. Colours show the increase in number of days for a given month when the local average sea ice conditions permit safe travel for projections of 2°C (left) and 4°C (right) of warming relative to 1°C of warming (~1 and 3°C above present day).

global warming relative to 1°C of global warming (approximately present day) are shown in Fig. 4. The timing of local changes to facilitate a longer increased access for resupply PC7 class ships depends heavily on the community location in the Canadian Arctic. Nunatsiavut communities have negligible changes because current ice conditions already facilitate near year-round access to resupply ships. However, almost all communities in Nunavik and southern Nunavut are projected to have substantial increases in access from January to June. When combined with a largely open water season through summer and fall, this results in near year-round shipping opportunities. Northern Nunavut will experience increased navigability during the shoulder seasons (November to January and May to July). The largest increases in navigability in the Canadian Arctic are expected to be in the Inuvialuit region and occur from July through December.

Changes in projected NIS (pleasure craft) shipping navigability for communities across the Canadian Arctic under 2 and 4°C of global warming are shown in Extended Data Fig. 1. As with the PC7 class ship, larger increases in navigability are more apparent under 4°C compared to 2°C of global warming. The largest increases in navigability occur in the Inuvialuit region during the summer months which is similar to the PC7 ship class. However, pleasure craft increases in navigability occur mainly during the summer months in Nunavut and Nunavik, whereas they occur during the shoulder seasons for the PC7 ship class. Nunatsiavut communities are expected to have substantially increased pleasure craft navigability during winter months.

Discussion

The transformation of major international trade routes from the Southern Ocean to the Arctic Ocean under projected climate

warming will have profound implications for economic development and environmental and cultural sustainability across the Canadian Arctic. Shipping companies will gain profitable operating days from increased open water availability to PC7 vessels under 2 and 4°C of global warming, particularly if operators are willing to take on elevated risk related to mobile ice that will persist and create additional hazards even within safe operational thresholds dictated by Polar Code regulations (Fig. 3). Specifically, an additional 2 months of operating time can be gained for the Arctic Bridge and about 1 month in the Beaufort Sea. For the Northwest Passage, the added risk for a PC7 class vessel only adds ~2 weeks of extra shipping days before 4°C (Fig. 3). It follows that a reasonable question to ask is to what extent will the desire to increase profit begin to push increased risk as open water and more mobile ice begin to coexist? Indeed, the *Crystal Serenity* successfully navigated the southern route of the Northwest Passage in 2016 and 2017 but has since stopped operations. Major marine disasters have been avoided in Arctic Canada but the risk potential for a situation similar to the *M.S. Explorer*⁴⁶ could arise with increasing operator risk. This is especially concerning considering the threat of hazardous multi-year ice flowing southward from the northern Canadian Arctic will remain even under 2 and 4°C of warming.

While less projected ice in the Northwest Passage could facilitate an increased amount of ship traffic^{7,8} (Fig. 3), a cautious approach is warranted with respect the practical and safe use of the Northwest Passage as a transport corridor. Local-scale ice advection processes (which are not well captured by coarse resolution climate models) pose hazardous conditions to transiting ships operating within the Canadian Arctic. The ice arches and bridges that have historically blocked the flow of thick Arctic Ocean multi-year sea ice southward into the Canadian Arctic for most of the year have weakened, resulting in increased southward ice advection into major shipping lanes^{39,47–49}. As a result, there are many regions where thick multi-year ice tends to accumulate within the Northwest Passage channels of the Canadian Arctic Archipelago⁵⁰, which climate model simulations do not capture. As summer Arctic sea ice extent recedes towards the northern coast of the Canadian Arctic Archipelago and Greenland due to warming temperatures (Fig. 2), the Transpolar Sea Route may become a more attractive (less risky) option for shipping compared to the Northwest Passage. Under such circumstances, some or most of the potential socio-economic benefits to northern communities from the use of the Northwest Passage could be lost, while at the same time the potential environmental and cultural risks would also be reduced. This dichotomy will most certainly present policy-related challenges for any new shipping routes, especially in Canada⁴⁹. The projected increases in accessibility in the Beaufort Sea as an alternative supply route that could connect to the Transpolar route could present more feasible options for improving food security and self-determined economic development in the region but only if managed effectively.

The expansion of shipping access highlighted in Figs. 2 and 3 has complex environmental and social impacts on communities across northern Canada. The direct economic benefits of increased shipping activity/efficiency are not always felt by northern communities but they absorb the risk associated with increased ship activity (local pollution, ecosystem impacts and so on). Impacts on resupply highlighted in Fig. 4 will matter greatly if changes are large enough to enable communities to receive resupply more than once per year. This will lead to lower food prices and lower rates of food insecurity in the region, with cascading implications for local health outcomes and reduced carbon emission associated with air shipments. While a longer period for ship-based northern community resupply is a potential benefit, this must be considered alongside shorter landfast ice seasons⁵¹, which have negative consequences for intercommunity travel and access to traditional hunting grounds. Even with increased community access and potentially increased

development, there are also physical changes that have negative implications in coastal communities. For example, projected decreases in sea ice extent are expected to facilitate increased winds and waves⁵², which could cause problems for coastal communities and infrastructure development across the Canadian Arctic. The LIA could become a last chance tourism destination for the Arctic and boost overall tourism in the Canadian Arctic. However, increased ship activity within the LIA region will pose ecosystem-related concerns, as it will be an important refuge for sea ice-dependent species⁵³.

A final consideration is that, although 2 and 4°C warming may facilitate more ship navigability, future changes in Canadian Arctic shipping activity may not be driven by physical changes in sea ice but instead by external socio-economic drivers which can be difficult to predict (for example, covid-19 impacts on tourism). This was previously identified in the Canadian Arctic whereby changes in shipping activity were associated with infrastructure development, economic activities and resource extraction¹⁵. As a result, there still remains considerable uncertainty as to how future sea ice changes and socio-economic drivers will combine to influence future shipping activity in and through the Canadian Arctic and its subsequent impact on communities.

Online content

Any methods, additional references, Nature Research reporting summaries, source data, extended data, supplementary information, acknowledgements, peer review information; details of author contributions and competing interests; and statements of data and code availability are available at <https://doi.org/10.1038/s41558-021-01087-6>.

Received: 22 October 2020; Accepted: 27 May 2021;
Published online: 8 July 2021

References

1. *Transport Volume of Worldwide Maritime Trade 1990–2016* (Statista Research Department, 2020); <https://www.statista.com/statistics/264117/tonnage-of-worldwide-maritime-trade-since-1990/> <http://bit.ly/2NDtBzW>
2. *World Bank Open Data* (World Bank, accessed March 2020); <https://data.worldbank.org/>
3. *Trade Overview* (World Bank, accessed March 2020); <https://www.worldbank.org/en/topic/trade/overview/>
4. Eaton, J., Kortum, S., Neiman, B. & Romalis, J. Trade and the global recession. *Am. Econ. Rev.* **106**, 3401–3438 (2016).
5. *Is Trade Good or Bad for the Environment?* (National Bureau of Economic Research, accessed March 2020); <https://www.nber.org/digest/nov02/w9021.html>
6. Stephenson, S., Smith, L. & Agnew, J. Divergent long-term trajectories of human access to the Arctic. *Nat. Clim. Change* **1**, 156–160 (2011).
7. Smith, L. C. & Stephenson, S. R. New Trans-Arctic shipping routes navigable by mid century. *Proc. Natl Acad. Sci. USA* **110**, E1191–E1195 (2013).
8. Melia, N., Haines, K. & Hawkins, E. Sea ice decline and 21st century trans-Arctic shipping routes. *Geophys. Res. Lett.* **43**, 9720–9728 (2016).
9. Brooks, M. & Frost, J. D. Providing freight services to remote Arctic communities: are there lessons for practitioners from services to Greenland and Canada's northeast? *Res. Transp. Bus. Manag.* **4**, 69–78 (2012).
10. Dawson, J. et al. Infusing local knowledge and community perspectives into the Low Impact Shipping Corridors: an adaptation to increased shipping activity and climate change in Arctic Canada. *Environ. Sci. Policy* **105**, 19–36 (2020).
11. Derksen, C. et al. in *Canada's Changing Climate Report* (eds Bush, E. & Lemmen, D.S.) Ch. 5 (Government of Canada, 2018).
12. Tivy, A. et al. Trends and variability in summer sea ice cover in the Canadian Arctic based on the Canadian Ice Service Digital Archive, 1960–2008 and 1968–2008. *J. Geophys. Res.* **116**, C03007 (2011).
13. Dawson, J., Pizzolato, L., Howell, S. E. L., Copland, L. & Johnston, M. E. Temporal and spatial patterns of ship traffic in the Canadian Arctic from 1990 to 2015. *Arctic* **71**, 15–26 (2018).
14. Eguiluz, V., Fernández-Gracia, J., Irigoien, X. & Duarte, C. M. A quantitative assessment of Arctic shipping in 2010–2014. *Sci. Rep.* **6**, 30682 (2016).
15. Pizzolato, L., Howell, S. E. L., Dawson, J., Laliberté, F. & Copland, L. The influence of declining sea ice on shipping activity in the Canadian Arctic. *Geophys. Res. Lett.* **43**, 12146–12154 (2016).

16. Dawson, J., Stewart, E. J., Johnston, M. E. & Lemieux, C. J. Identifying and evaluating adaptation strategies for cruise tourism in Arctic Canada. *J. Sustain. Tour.* **24**, 1425–1441 (2016).
17. Johnston, M., Dawson, J., De Souza, E. & Stewart, E. J. Management challenges for the fastest growing marine shipping sector in Arctic Canada: pleasure crafts. *Polar Rec.* **53**, 67–78 (2017).
18. Johnston, M. E., Dawson, J. & Maher, P. T. Strategic development challenges in marine tourism in Nunavut. *Resources* **6**, 25 (2017).
19. Bennett, M. M., Stephenson, S. R., Yang, Y., Bravo, M. T. & De Jonghe, B. The opening of the transpolar sea route: logistical, geopolitical, environmental, and socioeconomic impacts. *Mar. Policy* **121**, 104178 (2020).
20. Zeng, Q., Lu, T., Lin, K. C., Yuen, K. F. & Li, K. X. The competitiveness of Arctic shipping over Suez Canal and China–Europe railway. *Transp. Policy* **86**, 34–35 (2020).
21. Mahlstein, I. & Knutti, R. September Arctic sea ice predicted to disappear near 2°C global warming above present. *J. Geophys. Res.* **117**, D06104 (2012).
22. Screen, J. A. & Williamson, D. Ice-free Arctic at 1.5°C? *Nat. Clim. Change* **7**, 230–231 (2017).
23. Jahn, A. Reduced probability of ice-free summers for 1.5°C compared to 2°C warming. *Nat. Clim. Change* **8**, 409–413 (2018).
24. Sigmond, M., Fyfe, J. C. & Swart, N. C. Ice-free Arctic projections under the Paris Agreement. *Nat. Clim. Change* **8**, 404–408 (2018).
25. Gregory, J. M. et al. Recent and future changes in Arctic sea ice simulated by the HadCM3 AOGCM. *Geophys. Res. Lett.* **29**, 2175 (2002).
26. Winton, M. Do climate models underestimate the sensitivity of northern hemisphere sea ice cover? *J. Clim.* **24**, 3924–3934 (2011).
27. Notz, D. & Stroeve, J. Observed Arctic sea-ice loss directly follows anthropogenic CO₂ emission. *Science* **354**, 747–750 (2016).
28. Community, SIMIP Arctic sea ice in CMIP6. *Geophys. Res. Lett.* **47**, e2019GL086749 (2020).
29. IPCC *Climate Change 2013: The Physical Science Basis* (eds Stocker, T. F. et al.) (Cambridge Univ. Press, 2013).
30. Gillett, N. P., Arora, V. K., Matthews, D. & Allen, M. R. Constraining the ratio of global warming to cumulative CO₂ emissions using CMIP5 simulations. *J. Clim.* **26**, 6844–6858 (2013).
31. Tokarska, K. et al. The climate response to five trillion tonnes of carbon. *Nat. Clim. Change* **6**, 851–855 (2016).
32. *Adoption of the Paris Agreement* Report. No. FCCC/CP/2015/L. 9/Rev. 1, 21932 (UNFCCC, 2015).
33. *Polar Code Resources* (Lloyd's Register, accessed January 2021); <http://www.lr.org/en/resources-polar-code/>
34. *International Code for Ships Operating in Polar Waters (Polar Code)* (International Maritime Organization, accessed January 2021); <https://www.imo.org/en/OurWork/Safety/Pages/polar-code.aspx>
35. Chircop, A. The polar code and the Arctic marine environment: assessing the regulation of the environmental risks of shipping. *Int. J. Mar. Coast. Law* **35**, 533–569 (2020).
36. Fraser, D. in *Governance of Arctic Shipping Rethinking Risk, Human Impacts and Regulation* (eds Chircop, A. et al.) 285–300 (Springer, 2020).
37. Comiso, J. C. Large decadal decline of the Arctic multiyear ice cover. *J. Clim.* **25**, 1176–1193 (2012).
38. Babb, D. G., Galley, R. J., Barber, D. G. & Rysgaard, S. Physical processes contributing to an ice free Beaufort Sea during September 2012. *J. Geophys. Res. Oceans* **121**, 267–283 (2016).
39. Moore, G. W. K. & McNeil, K. The early collapse of the 2017 Lincoln Sea ice arch in response to anomalous sea ice and wind forcing. *Geophys. Res. Lett.* **45**, 8343–8351 (2018).
40. *Oil and Gas Exploration and Development Activity Forecast: Canadian Beaufort Sea 2013–2028* (LTLC Consulting and Salmo Consulting Inc., accessed 21 October 2020); https://www.beaufortsea.ca/wp-content/uploads/2012/03/NCR-5358624-v4-BREA_-_FINAL_UPDATE_-_EXPLORATION_AND_ACTIVITY_FORECAST_-_MAY_2013.pdf
41. Stroeve, J., Barrett, A., Serreze, M. & Schweiger, A. Using records from submarine, aircraft and satellites to evaluate climate model simulations of Arctic sea ice thickness. *Cryosphere* **8**, 1839–1854 (2014).
42. Howell, S. E. L., Laliberté, F., Kwok, R., Derksen, C. & King, J. Landfast ice thickness in the Canadian Arctic Archipelago from observations and models. *Cryosphere* **10**, 1463–1475 (2016).
43. Laliberté, F., Howell, S. E. L. & Kushner, P. J. Regional variability of a projected sea ice-free Arctic during the summer months. *Geophys. Res. Lett.* **43**, 256–263 (2016).
44. Smith, A. & Jahn, A. Definition differences and internal variability affect the simulated Arctic sea ice melt season. *Cryosphere* **13**, 1–20 (2019).
45. Andrews, J., Babb, D., Barber, D. G., Deming, J. W. & Ackley, S. F. Climate change and sea ice: shipping accessibility on the marine transportation corridor through Hudson Bay and Hudson Strait (1980–2014). *Elem. Sci. Anth.* **5**, 15 (2017).
46. Stewart, E. J. & Draper, D. The sinking of the M.S. Explorer: implications for cruise tourism in Arctic Canada. *Arctic* **61**, 224–228 (2008).
47. Barber, D. G. et al. Increasing mobility of high Arctic Sea ice increases marine hazards off the east coast of Newfoundland. *Geophys. Res. Lett.* **45**, 2370–2379 (2018).
48. Howell, S. E. L. & Brady, M. The dynamic response of sea ice to warming in the Canadian Arctic Archipelago. *Geophys. Res. Lett.* **46**, 13119–13125 (2019).
49. Vincent, R. F. A study of the North Water polynya ice arch using four decades of satellite data. *Sci. Rep.* **9**, 20278 (2019).
50. Haas, C. & Howell, S. E. L. Ice thickness in the northwest passage. *Geophys. Res. Lett.* **42**, 7673–7680 (2015).
51. Cooley, S. W. et al. Coldest Canadian Arctic communities face greatest reductions in shorefast sea ice. *Nat. Clim. Change* **10**, 533–538 (2020).
52. Casas-Prat, M. & Wang, X. Sea ice retreat contributes to projected increases in extreme Arctic ocean surface waves. *Geophys. Res. Lett.* **47**, e2020GL088100 (2020).
53. Lange, B. A. et al. Contrasting ice algae and snow-dependent irradiance relationships between landfast first-year and multi-year sea ice. *Geophys. Res. Lett.* **46**, 10834–10843 (2019).

Publisher's note Springer Nature remains neutral with regard to jurisdictional claims in published maps and institutional affiliations.

© Crown 2021

Methods

Model data. We use a single model initial condition large ensemble of 40 realizations from the Community Earth System Model version 1 (CESM1). All ensemble members were forced with identical historical emissions from 1920 to 2005 followed by a high carbon emissions future scenario from 2006 to 2100 (Representative Concentration Pathway 8.5). Further details of the model and ensemble experiment are described in Kay et al.⁵⁴. While individual model realizations are subject to the effects of internal variability (Extended Data Fig. 2), we largely eliminate this component of uncertainty by averaging over the large number of ensemble members.

Model representation of sea ice. In general, CESM1 reasonably captures the Arctic mean state, trends and variability related to sea ice concentration^{55–58}. Most climate models (including CESM1) tend to underestimate the sensitivity of sea ice to global warming, a persistent issue in several generations of models^{26,28,59}. This deficiency may indicate that our results are conservative; however, navigability is likely to be more strongly affected by the representation of simulated melt and growth processes and thereby sea ice thickness⁶⁰. Labe et al.⁶¹ show that while CESM1 has high thickness bias for the Arctic mean compared to estimates from the Pan-Arctic Ice Ocean Modeling and Assimilation System (PIOMAS), all ensemble members closely reproduce the timing of the seasonal cycle. They also demonstrate that CESM1 compares well with PIOMAS in terms of the regional distribution of sea ice thickness and has similar patterns of spatial variability. Even more importantly, rates of decline of both March and September sea ice thickness over the recent historical period are well captured by the ensemble mean of the simulations (see Fig. 9 in ref. ⁶¹). On the basis of comprehensive comparisons with observations^{41–43}, we expect the most problematic regions to contain extensive multi-year ice or a mix of multi-year and seasonal ice (for example, the higher latitude regions of the Canadian Arctic Archipelago and the northern route of the Northwest Passage). Such regions may have less realistic projections of sea ice thickness, as the models tend to overestimate the thickness of multi-year ice which is present historically. This bias implies that projected shipping impacts in these regions will be more uncertain at intermediate time scales (for example, 2°C of warming or ~2050). With increased warming resulting in a thinner, more seasonal ice cover, the models are likely to become more representative.

Relating simulated sea ice thickness to navigability. Navigability conditions are determined independently in each realization using daily sea ice thickness over the 1960–2100 period. Ice thickness is converted into RIO values using POLARIS. This system weights the selection of ice types and corresponding ice thicknesses in a given region to determine the threshold of acceptable and unacceptable risk to a particular class of ship. Specifically:

$$\text{RIO} = C_1\text{RV}_1 + C_2\text{RV}_2 + \dots + C_N\text{RV}_N,$$

where $C_1 \dots C_N$ are the relative proportions of 12 different specified ice types (Supplementary Table 1) within the considered region and $\text{RV}_1 \dots \text{RV}_N$ are the corresponding risk index values, which differ according to vessel class. Each of the 12 ice types has a distinct, non-overlapping thickness range associated with it progressing from zero thickness ('no ice') to 3 m or more ('multi-year ice'). The risk index values assigned to each ice type function as weights and range from -8 to +3 depending on the ice type/ice thickness and the class of ship being considered. To simplify calculations in operational use, the relative proportions ($C_1 \dots C_N$) of ice types contained within a given region are measured in units of 'tenths' (that is, five-tenths means the ice type occupies half of the region), yielding risk index outcome (RIO) values that range from -80 to +30. The POLARIS framework specifies that positive RIOs are considered indicative of normal operating conditions and present an acceptable level of risk for ship navigation. Negative RIOs indicate unacceptable risk and such regions should be avoided. In addition to this simple 'go or no-go' threshold, POLARIS also allow for restricted navigation between -10 and 0. These RIOs represent conditions that pose elevated operational risk but at a level which may be acceptable for certain vessel classes and/or under some operating conditions. For Fig. 2, only the threshold $\text{RIO} \geq 0$ is used. For Fig. 3, thresholds of both $\text{RIO} \geq 0$ and $\text{RIO} \geq -10$ are used as described in the figure caption.

We calculate RIOs for two types of regions: individual model grid cells and composite regions comprising multiple grid cells, representative of typical Canadian trade routes. For individual model grid cells only the mean ice thickness is available from the model so a single ice type corresponding to this mean thickness is assumed to completely cover the entire grid cell (including the possibility of zero thickness/'no ice' type). Hence, the entire grid cell is either navigable or not for a particular vessel class. For the larger composite regions, the proportions of a given ice type are determined by the fraction of the total region covered by grid cells of ice within the associated thickness range. All of the ice types present within the region are summed together as in the equation above to determine a single RIO considered to apply to the region as a whole.

Season length as a function of warming. The RIO calculations are performed for four different ship classes, for all days between 1960 and 2100 and for all 40 model realizations (individually for all ocean grid cells as well as for the four composite regions). The resulting RIOs are used to determine, for a given ice year (defined to begin 1 April and extend until 31 March of the following calendar

year), the first day and last day that a particular grid cell or region is continuously navigable as well as the total duration over which the selected area is navigable. We calculate ensemble means of the first and last days of the navigable season and the season length. Ice years over which the considered area is never navigable are not considered in calculating the ensemble mean values for first and last days of the season but are considered in the ensemble mean season length by assigning a season length of zero days. For local community conditions determining resupply and tourism access, we present ensemble mean navigability results using the nearest model ocean grid cell. In the Supplementary Information, we evaluate how simulated navigability characteristics (season length and first/last days of shipping season) for the Canadian trade routes compare with quantities calculated using satellite observations available over the 1979–2018 period.

We produce maps of season length at a given level of global mean surface warming by calculating the ensemble mean over the selection of ice years that each given realization crossed each particular warming threshold. We calculate the warming of each realization for a given calendar year from the global mean surface temperature difference with respect to pre-industrial values. The latter is calculated as the 200-yr average global mean surface temperature from the corresponding pre-industrial control run of the CESM1 large ensemble. Individual maps for a given ship class and warming level are calculated on the CESM ice-model grid; the resulting ensemble mean is regridded to a regular 0.5×0.5 longitude–latitude grid.

Data availability

The original model data used in this analysis are available from the Climate Data Gateway at NCAR (repository identifier, <https://doi.org/10.17616/R37N41>; data set identifier, <https://doi.org/10.5065/d6j101d1>). Derived data supporting the findings of this study are available from the corresponding author on request. The CISDA (historical ice data presented in Supplementary Information) are available online from the Canadian Ice Service (CIS; <https://www.canada.ca/en/environment-climate-change/services/ice-forecasts-observations/latest-conditions/archive-overview.html>).

Code availability

The code associated with this paper is available from GitHub: <https://github.com/mudryk/arctic-navigability-POLARIS>.

References

- Kay, J. E. et al. The Community Earth System Model (CESM) Large Ensemble Project: a community resource for studying climate change in the presence of internal climate variability. *Bull. Am. Meteor. Soc.* **96**, 1333–1349 (2015).
- Barnhart, K., Miller, C., Overeem, I. & Kay, J. Mapping the future expansion of Arctic open water. *Nat. Clim. Change* **6**, 280–285 (2019).
- DeRepentigny, P., Jahn, A., Holland, M. M. & Smith, A. Arctic sea ice in two configurations of the CESM2 during the 20th and 21st centuries. *J. Geophys. Res. Oceans* **125**, e2020JC016133 (2020).
- England, M., Jahn, A. & Polvani, L. Nonuniform contribution of internal variability to recent Arctic sea ice loss. *J. Clim.* **32**, 4039–4053 (2019).
- Jahn, A., Kay, J. E., Holland, M. M. & Hall, D. M. How predictable is the timing of a summer ice-free Arctic? *Geophys. Res. Lett.* **43**, 9113–9120 (2016).
- Rosenblum, E. & Eisenman, I. Sea ice trends in climate models only accurate in runs with biased global warming. *J. Clim.* **30**, 6265–6278 (2017).
- Massonnet, F. et al. Arctic sea-ice change tied to its mean state through thermodynamic processes. *Nat. Clim. Change* **8**, 599–603 (2018).
- Labe, Z., Magnusdottir, G. & Stern, H. Variability of Arctic sea ice thickness using PIOMAS and the CESM Large Ensemble. *J. Clim.* **31**, 3233–3247 (2018).

Acknowledgements

Model data was produced thanks to the CESM Large Ensemble Community Project and supercomputing resources provided by NSF/CISL/Yellowstone. J.D. acknowledges funding from the following grants: 100 (ArcticNet), 2-02-03-018.1 (MEOPAR; Irving Shipbuilding Inc.), 2-02-03-039.1 (MEOPAR; ClearSeas), 950-225044 (Canada Research Chairs).

Author contributions

J.D., S.H. and C.D. conceptualized the study. L.M. performed the analysis and created Figs. 2–4. J.D., S.H., C.D. and T.Z. advised on analysis. M.B. created Fig. 1. All authors contributed to writing and editing the paper.

Competing interests

The authors declare no competing interests.

Additional information

Extended data is available for this paper at <https://doi.org/10.1038/s41558-021-01087-6>.

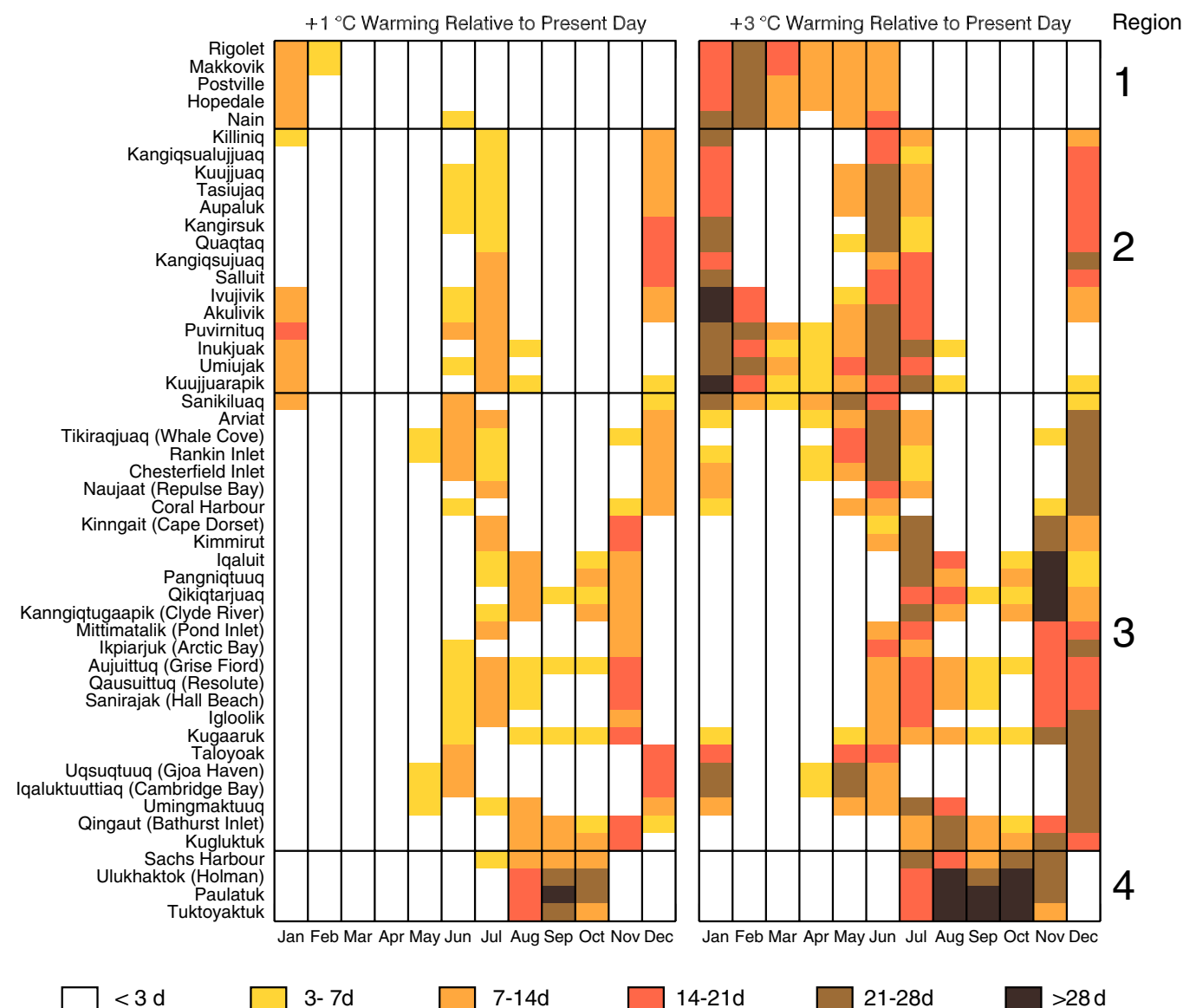
Supplementary information The online version contains supplementary material available at <https://doi.org/10.1038/s41558-021-01087-6>.

Correspondence and requests for materials should be addressed to L.R.M.

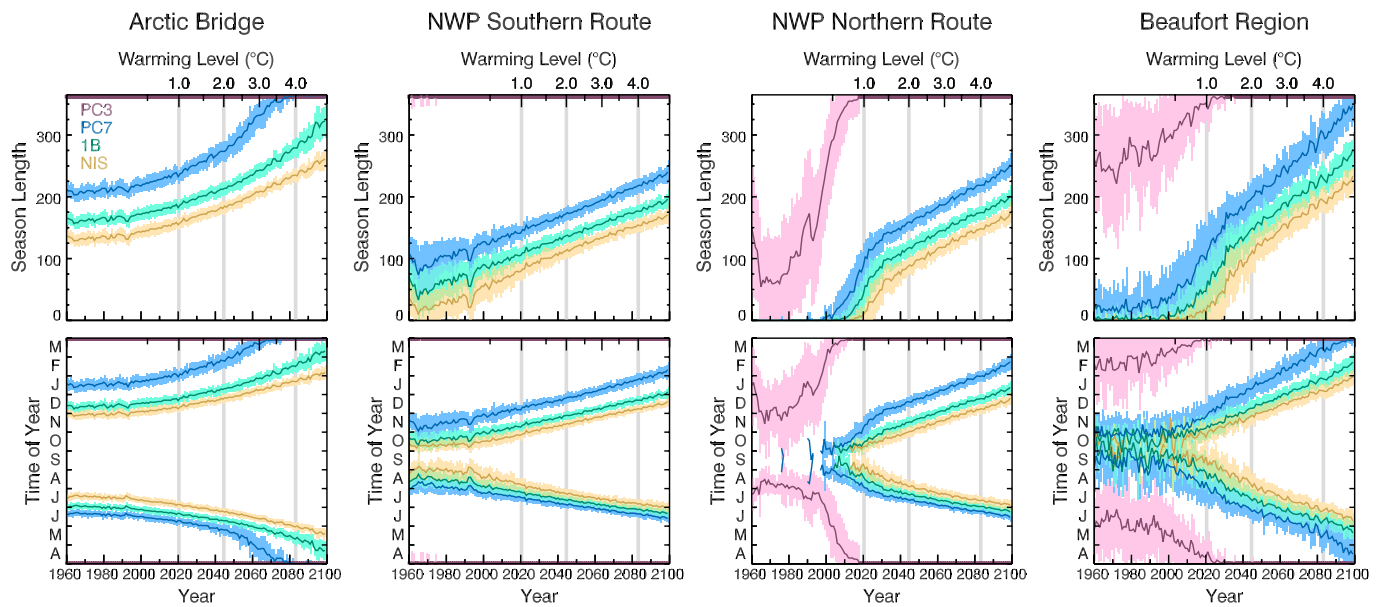
Peer review information *Nature Climate Change* thanks Henry Huntington and the other, anonymous, reviewer(s) for their contribution to the peer review of this work.

Reprints and permissions information is available at www.nature.com/reprints.

Northern Community Increases in Pleasure Craft Navigability



Extended Data Fig. 1 | Changes in timing of pleasure craft navigability for localized regions near Northern Communities. Colours show the increase in number of days for a given month when the average local sea ice conditions permit safe travel for projections of 2 °C (left) and 4 °C (right) of warming relative to 1 °C of warming (approximately 1 °C and 3 °C above present day).



Extended Data Fig. 2 | Spread due to natural variability in evolution of four Canadian shipping regions. Shipping season length (top row), first/last day of possible transit (middle row), and annual navigation probability (bottom row) shown for four Canadian shipping regions and four ship classes: PC3 (magenta), PC7 (blue), 1B (green), and NIS (yellow). Solid lines show ensemble mean values; shading shows spread about the mean due to natural variability. Spread is calculated independently at each year as the standard deviation among the 40 ensemble members above and below the ensemble mean. Vertical grey lines indicate ensemble mean timing of 1°C, 2°C, and 4°C warming thresholds relative to pre-industrial values.